frontiers | Frontiers in Earth Science

TYPE Original Research
PUBLISHED 15 August 2022
DOI 10.3389/feart.2022.953364

Check for updates

OPEN ACCESS

EDITED BY
Hossein Azizi,
University of Kurdistan, Iran

REVIEWED BY
Paterno Castillo,
University of California, San Diego, United States
Li-Qun Dai,
University of Science and Technology of China, China

*CORRESPONDENCE
Lu-Lu Hao,
haolulu@gig.ac.cn
Yue Qi,
qiyue2233@163.com

SPECIALTY SECTION
This article was submitted to Petrology, a section of the journal Frontiers in Earth Science

RECEIVED 26 May 2022
ACCEPTED 30 June 2022
PUBLISHED 15 August 2022

CITATION
Zhang M-Y, Hao L-L, Wang Q, Qi Y and Ma L (2022), B–Sr–Nd isotopes of Miocene trachyandesites in Lhasa block of southern Tibet: Insights into petrogenesis and crustal reworking. *Front. Earth Sci.* 10:953364. doi: 10.3389/feart.2022.953364

COPYRIGHT
© 2022 Zhang, Hao, Wang, Qi and Ma. This is an open-access article distributed under the terms of the Creative Commons Attribution License (CC BY). The use, distribution or reproduction in other forums is permitted, provided the original author(s) and the copyright owner(s) are credited and that the original publication in this journal is cited, in accordance with accepted academic practice. No use, distribution or reproduction is permitted which does not comply with these terms.

B–Sr–Nd isotopes of Miocene trachyandesites in Lhasa block of southern Tibet: Insights into petrogenesis and crustal reworking

Miao-Yan Zhang[1,2], Lu-Lu Hao[1,3]*, Qiang Wang[1,2,3], Yue Qi[1,3]* and Lin Ma[1,3]

[1]State Key Laboratory of Isotope Geochemistry, Guangzhou Insititute of Geochemistry, Chinese Academy of Sciences, Guangzhou, China, [2]College of Earth and Planetary Sciences, University of Chinese Academy of Sciences, Beijing, China, [3]CAS Center for Excellence in Deep Earth Science, Guangzhou, China

Adakitic rocks at continental collisional zones have important implications for understanding the mechanism of crustal reworking. The Himalayan–Tibetan orogen, built by India–Asia collision and Indian continental plate subduction, is one of the most prominent Cenozoic continent–continent collision zones, and Cenozoic post-collisional adakitic rocks widely occur in the Lhasa block of southern Tibet. Numerous studies have suggested that the adakitic granitoids in the eastern Lhasa block were derived from partial melting of a juvenile crust and post-collisional mantle-derived ultrapotassic magmas significantly contributed to this crustal reworking by energy and mass transfer. However, the genesis of adakitic rocks in the western Lhasa block remains highly debated, hindering our understanding of crustal reworking in the whole Lhasa block. Here, we report zircon U–Pb age and whole-rock major, trace elemental and Sr–Nd–B isotopic compositions for the Sailipu trachyandesites in the western Lhasa block. Zircon U–Pb dating yields an eruption age of ~22 Ma. These trachyandesites are high-K calc-alkaline and exhibit intermediate SiO_2 (56.9–59.6 wt.%) and low MgO (2.3–4.2 wt.%) contents, low K_2O/Na_2O (0.8–1.1) ratios, enrichment in light rare earth elements (LREEs), and depletion in heavy REEs (HREEs) with negligible Eu and Sr concentration anomalies. They have high Sr (1080–1593 ppm) and low Y (14.0–26.8 ppm) and Yb (1.08–1.48 ppm) contents, with relatively high Sr/Y (46–95) and La/Yb (46–77) ratios showing adakitic affinities. These Sailipu adakitic rocks display $\delta^{11}B$ values of −9.7 to −2.7‰, which are higher than those of mid-ocean ridge basalts (MORBs) but similar to those of arc lavas, indicating contributions from the juvenile crust. However, they have more geochemically enriched Sr–Nd isotopes ($^{87}Sr/^{86}Sr_{(i)}$ = 0.7092–0.7095, $\varepsilon_{Nd}(t)$ = −8.09 to −7.25) than the juvenile crust, indicating contributions from ultrapotassic magmas. Thus, the Sailipu adakitic rocks were likely generated by the interaction between the juvenile lower crust and underplated ultrapotassic magmas. Combined with adakitic magmatism in the eastern Lhasa block, we suggest that magma underplating and subsequent crust–mantle mixing could have been a common and important process that induced the reworking of juvenile crust

beneath southern Tibet. This process may be related to the foundering of the subducted Indian continental slab.

KEYWORDS

B isotopes, adakitic rocks, post-collisional magmatism, crustal reworking, Tibetan Plateau (TP)

Introduction

Adakites were originally suggested to occur in modern convergent margins where young and hot oceanic slabs (≤25 Ma) are being subducted (Defant and Drummond, 1990). They are characterized by enrichment in light rare earth elements (LREEs) and Sr, strong depletion in heavy REEs (HREEs), and high Sr/Y and La/Yb ratios (e.g., Castillo, 2012). However, an increasing number of studies have identified adakitic or adakite-like rocks in Cenozoic continental collisional zones (e.g., Chung et al., 2003; Hou et al., 2004; Wang et al., 2005). These adakitic rocks were mainly derived from partial melting of thickened lower crust. Therefore, they have important implications for understanding the mechanism of crustal reworking in continental collisional zones.

The well-known Himalayan–Tibetan orogen, one of the prominent Cenozoic continent–continent collisional zones, is the consequence of Neo-Tethyan oceanic subduction, India–Asia continental collision, and Indian continental plate subduction (Yin and Harrison, 2000). Post-collisional magmatic rocks are widely distributed in the Lhasa block of southern Tibet, including potassium-rich (potassic and ultrapotassic) volcanic rocks (e.g., Guo et al., 2015; Liu et al., 2015; Tian et al., 2020) and adakitic extrusive/intrusive rocks (e.g., Chung et al., 2003; Hou et al., 2004; Chung et al., 2005; Chung et al., 2009; Xu et al., 2010). The adakitic rocks mainly occur in the eastern Lhasa block. Numerous recent studies have suggested that they were derived from partial melting of a juvenile crust with contribution from post-collisional mantle-derived ultrapotassic magmas (e.g., Yang et al., 2015; Wang et al., 2018; Hao et al., 2021). This indicates that underplating of ultrapotassic magmas induced the reworking of juvenile crust in the eastern Lhasa block. However, the scarcity of adakitic rocks in the western Lhasa block draws much less attention, and their genesis remains unclear. Different from adakitic rocks in the eastern Lhasa block that show relatively geochemically depleted Sr–Nd isotopic compositions, adakitic rocks in the western Lhasa block generally show much more enriched Sr–Nd isotopes, which were previously ascribed to their origination from an ancient lower crust (Guo et al., 2007; Liu et al., 2017; Hao et al., 2019a). However, it is unclear whether these geochemically enriched signatures could be coming from ultrapotassic magmas. It is also unclear whether the juvenile crust contributed to the formation of adakitic rocks in the western Lhasa block, given that ultrapotassic magmas may have obscured the signatures of juvenile crust. These uncertainties hinder our understanding of mechanism of crustal reworking in the western Lhasa block of southern Tibet.

Boron isotopes have the potential to discriminate between ancient lower crust, ultrapotassic magma, and juvenile crust. Continental crust mainly consists of crystalline basement and continental sediments which typically have low $\delta^{11}B$ (−9.1 ± 2.4‰, Trumbull and Slack, 2017). Recent studies have shown that post-collisional ultrapotassic rocks have much lower $\delta^{11}B$ values than depleted mantle and MORBs ($\delta^{11}B$ = −7.1 ± 0.9‰; Marschall et al., 2017). For example, the Miocene K-rich rocks in western Anatolia have low $\delta^{11}B$ values down to −31‰ (Palmer et al., 2019), and post-collisional ultrapotassic rocks in the Lhasa block also have low $\delta^{11}B$ values from −20.5 to −10.3‰ (Hao et al., 2022). In contrast, subducted oceanic slabs have overall positive B isotopic ratios (altered oceanic crust: $\delta^{11}B$ = 0~ +18‰; marine sediments: $\delta^{11}B$ = +2~ +26‰; Marschall, 2017). Slab-derived fluids preferentially mobilize B, especially ^{11}B, resulting in a metasomatized mantle with higher B concentrations, B/Nb ratios, and $\delta^{11}B$ values than depleted mantle and MORBs. The juvenile crust or arc magmas formed during oceanic subduction thus have high $\delta^{11}B$ values ($\delta^{11}B$ = −9 to +16‰; De Hoog and Savov, 2017).

In this study, we report zircon U–Pb age and whole-rock major, trace elemental and Sr–Nd–B isotopic compositions for the post-collisional adakitic trachyandesites in the Sailipu basin in the western Lhasa block. These geochemical data can offer important opportunities to constrain the petrogenesis of these adakitic rocks and further to decipher the mechanism of crustal reworking in continental collision zones.

Geological background and samples

The Himalayan–Tibetan orogen consists mainly of the Songpan–Ganze, Qiangtang, Lhasa, and Himalaya blocks, from north to south (Yin and Harrison, 2000). The Lhasa block in southern Tibet is separated from the Qiangtang block by the Bangong–Nujiang suture zone (BNS) to the north and from the Himalayas by the Indus–Yarlung Zangbo suture zone (IYZS) to the south. The Lhasa block is further divided into northern, central, and southern sub-blocks, separated by the Shiquan River–Nam Tso Mélange Zone (SNMZ) and Luobadui–Milashan Fault (LMF), respectively (Figure 1A) (Zhu et al., 2013). Bangong–Nujiang oceanic subduction and closure produced early Jurassic–late Cretaceous magmatism in northern and central Lhasa

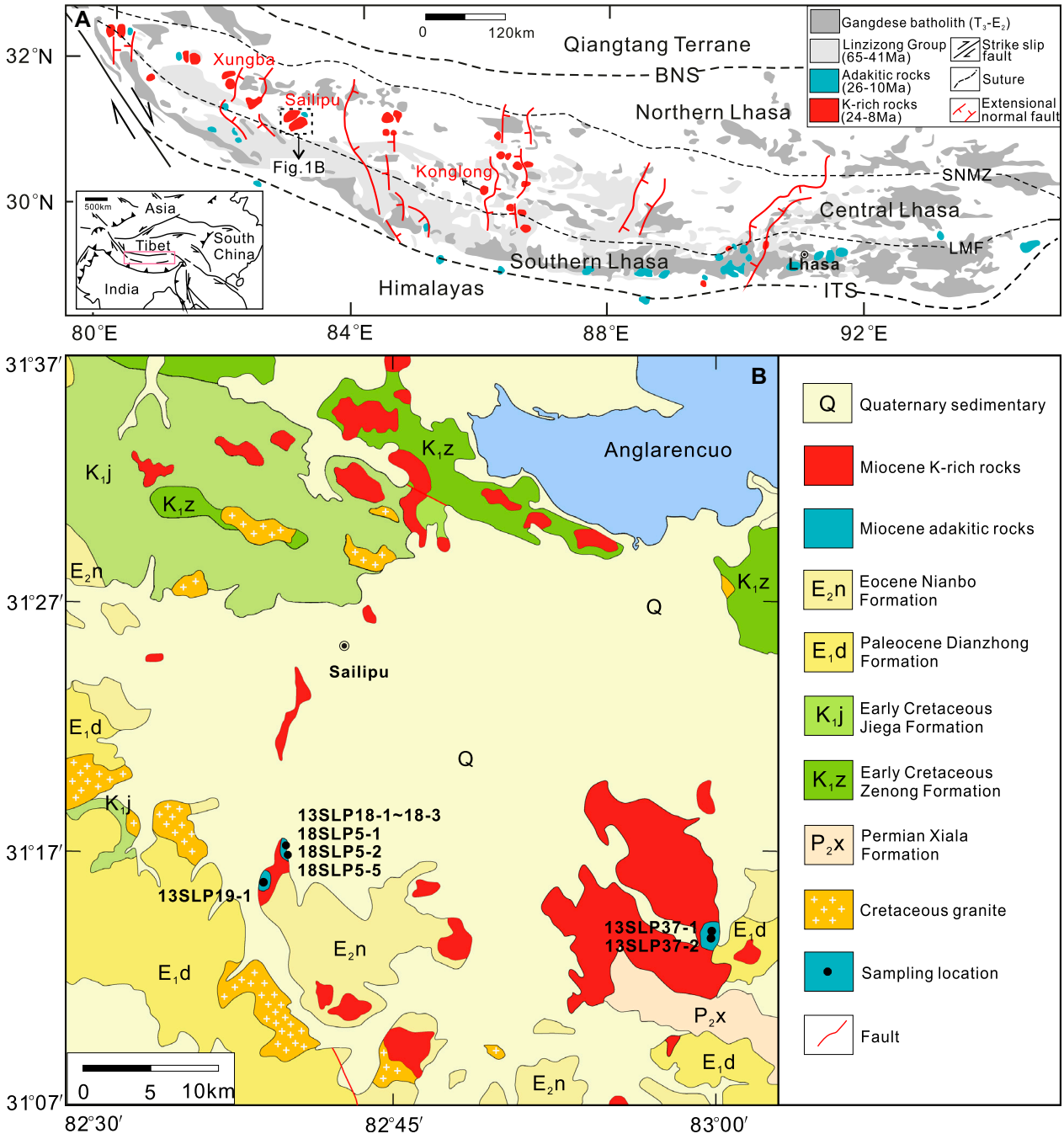

FIGURE 1
(A) A simplified geologic map of the Lhasa block showing distribution of Cenozoic magmatic rocks, modified from Guo et al. (2015). BNS, Bangong–Nujiang suture; ITS, Indus–Yarlung Zangbo suture; SNMZ, Shiquan River–Nam Tso Mélange Zone; LMF, Luobadui–Milashan Fault; T3, late Triassic; E2, Eocene. **(B)** Regional geological map of the Sailipu area in the western Lhasa block.

sub-blocks, while Neo-Tethys oceanic subduction yielded late Triassic–Cretaceous magmatism and Paleogene Linzizong volcanic rocks and coeval batholiths in southern and central Lhasa sub-blocks (Zhu et al., 2011). Moreover, previous studies have shown that the central Lhasa sub-block was once a microcontinent with Archean basement, whereas southern and northern sub-blocks are characterized by the presence of juvenile crust due to the southward subduction of Bangong–Nujiang Ocean and northward subduction of Neo-Tethys Ocean, respectively (Zhu et al., 2011).

The Lhasa–India continental collision was considered to have occurred in early Cenozoic (Hu et al., 2015). After the Neo-Tethys oceanic slab broke off at ~50–45 Ma, southern Tibet evolved into a post-collisional setting. Post-collisional magmatism in the Lhasa block occurred since Oligocene and mainly consisted of potassic and ultrapotassic volcanic rocks (e.g., Chung et al., 2005; Zhao et al., 2009; Guo et al., 2013; Guo et al., 2015; Liu et al., 2017; Tian et al., 2020) and adakitic intrusions (e.g., Chung et al., 2003; Guo et al., 2007; Zheng et al., 2012), which occurred mainly in western and eastern Lhasa blocks, respectively. Adakitic lavas are rare in the western Lhasa block.

In this study, we focus on the post-collisional high-K calc-alkaline lava samples from the Sailipu area of western Lhasa block (Figure 1A). Numerous researchers have studied the Sailipu potassic and ultrapotassic rocks (Wang et al., 2008; Wang et al., 2014; Zhao et al., 2009; Liu et al., 2011; Chen et al., 2012; Liu et al., 2014; Cheng and Guo, 2017; Tian et al., 2020). The high-K calc-alkaline lavas spatially co-exist with the potassic and ultrapotassic rocks (Figure 1B). All the samples analyzed are fresh. They show typical porphyritic texture with phenocrysts of clinopyroxene and minor plagioclase (Supplementary Figure S1) and, thus, are typical trachyandesites. The groundmass consists mainly of microcrystalline clinopyroxene, plagioclase, and opaque minerals.

Analytical methods

All samples were cleaned of weathered surfaces, crushed to small fragments, and washed with Milli-Q water before the finial preparation for each type of analysis. All analyses were conducted in the State Key Laboratory of Isotope Geochemistry (SKLaBIG), Guangzhou Institute of Geochemistry, Chinese Academy of Sciences (GIG CAS).

Zircon U–Pb dating

Zircons were concentrated by heavy liquid and magnetic separation techniques. Zircon grains were handpicked under a binocular microscope and mounted in an epoxy resin disc with standard samples. Transmitted and reflected light micrographs as well as cathodoluminescence (CL) images were taken to inspect internal structures, inclusions, and physical defects in individual zircons prior to selecting positions for *in situ* U–Pb analyses. Zircon U–Pb analyses were determined using a CAMECA IMS 1280-HR secondary-ion mass spectrometer (SIMS) at the SKLaBIG, GIG CAS, using the analytical procedures described by Li et al. (2009). The ellipsoidal spot is about 20 μm × 30 μm in size. Zircon U–Th–Pb isotopic ratios were measured relative to the standard zircon Plešovice (Sláma et al., 2008). A secondary standard zircon Qinghu, which was used to monitor the reliability of the whole procedure, yielded concordant ages of 159.5 ± 2.4 Ma, consistent with the certified age of 159.5 ± 0.2 Ma (Li et al., 2013).

Whole-rock geochemistry

Whole-rock geochemical analysis required samples to be powdered to ~200 mesh with an agate mortar and pestle. Whole-rock major element oxides were analyzed in fused glass beads using a Rigaku RIX 2000 X-ray fluorescence spectrometer (XRF) at the SKLaBIG. Analytical procedures used are similar to those described by Li et al. (2005), and the analytical uncertainties are between 1 and 5%. Trace elemental compositions were determined using a Perkin-Elmer ELAN 6000 inductively coupled plasma-mass spectrometry (ICP-MS) at the SKLaBIG following the procedures described by Li et al. (2006); the analytical precision is typically better than 5%. The whole-rock Sr and Nd isotopic analyses were determined on a Neptune multi-collector (MC) ICP-MS, using the analytical procedures described by Li et al. (2004). All measured Sr and Nd isotopic ratios were corrected for fractionation of $^{87}Sr/^{86}Sr$ = 0.1194 and $^{143}Nd/^{144}Nd$ = 0.7219, respectively. The $^{87}Sr/^{86}Sr$ ratio of the standard NBS SRM 987 and the $^{143}Nd/^{144}Nd$ ratio of the standard Shin Etsu JNdi-1 were 0.710249 ± 17 (n = 5, 2σ) and 0.512113 ± 10 (n = 10, 2σ), respectively. The basaltic standard BHVO-2 was analyzed as unknown to monitor ion-exchange chromatographic purification and yielded an $^{87}Sr/^{86}Sr$ ratio of 0.703508 ± 22 (2σ) and an $^{143}Nd/^{144}Nd$ ratio of 0.512989 ± 10 (2σ), consistent with the certified values of $^{87}Sr/^{86}Sr$ = 0.703481 ± 20 and $^{143}Nd/^{144}Nd$ = 0.512983 ± 10, respectively (Weis et al., 2005).

Boron isotopic ratios and B concentrations of aliquots of the same solutions were measured by MC-ICP-MS and ICP-MS, respectively, applying the analytical procedure described by Wei et al. (2013). Powdered samples (150 mg) were weighed into a pre-cleaned 15 ml polypropylene (PP) centrifugal tube and digested with mannitol, H_2O_2, and HF at a constant temperature of 50–55°C for 15 days. Then, about 10 ml B-free Milli-Q deionized water was added to each tube, and the tubes were shaken and centrifuged for 10 min. The supernatant was collected for chromatographic purification. Boron was purified using a single column packed with pre-conditioned 20 ml Bio-Rad AG MP-1 strong anion exchange resin. The eluted boron was collected, dried at a temperature <55°C, and re-dissolved to 1.5 ml with Milli-Q water. A 0.1 ml aliquot of this 1.5 ml solution was re-diluted to 4 ml and taken for boron concentration measurement. The internal precision of measured B concentration was better than 3% (RSD). The basaltic standards B-5, JB-2, and JB-3 were measured as unknowns with our samples, yielding B concentrations of 11.05, 29.04, and 19.15 ppm, respectively. Boron isotope measurements were performed in the sample-standard-bracketing (SSB) mode. The internal precision for $\delta^{11}B$ was better than ±0.05‰ (2σ), and the external precision for $\delta^{11}B$ was better than ±0.30‰ (2σ) estimated by the long-term results of SRM 951 (Wei et al., 2013). The measured average $\delta^{11}B$ for basaltic standards such as B-5, JB-2, and JB-3 was −3.87 ± 0.04‰ (2σ, n = 3), 7.60 ± 0.05‰ (2σ, n = 2),

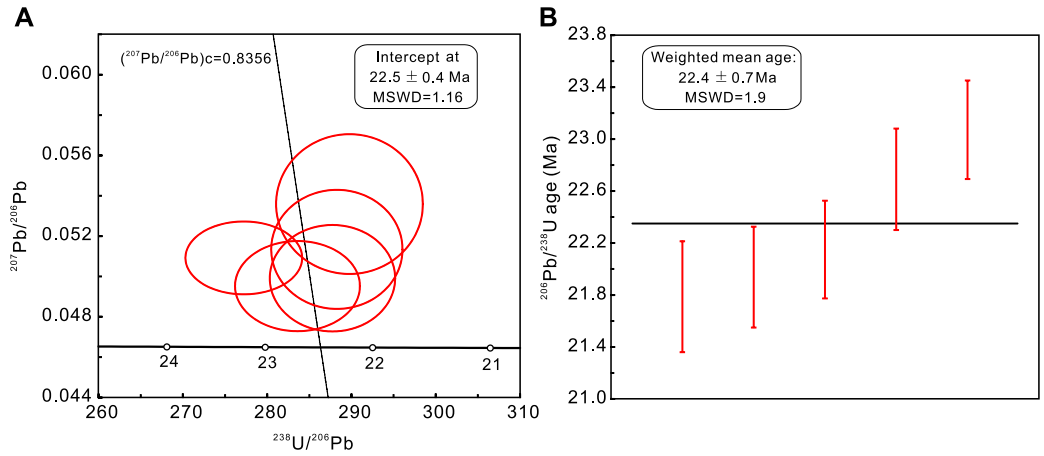

FIGURE 2
(A) Zircon U–Pb concordia age diagram for Sailipu high-K calc-alkaline trachyandesites (sample 18SLP5-1). **(B)** Weighted mean age.

and 6.67 ± 0.04‰ (2σ, $n = 3$), respectively, which are consistent with the published values within analytical errors (Wei et al., 2013).

Results

SIMS zircon U–Pb geochronology

Zircon U–Pb age data are presented in Supplementary Table S1. The analyzed zircon grains from the Sailipu trachyandesite sample (18SLP5-1) have variable U (186–573 ppm) and Th (18–361 ppm) contents, with Th/U ratios ranging from 0.05 to 1.94, indicating a magmatic origin. The calculated concordia age is 22.5 ± 0.4 Ma and the weighted average age is 22.4 ± 0.7 Ma (Figure 2), suggesting that the Sailipu trachyandesite formed in early Miocene, which is coeval with the ultrapotassic rocks in the western Lhasa block (e.g., the Xungba basin, Miller et al., 1999; Liu et al., 2011; Konglong area, Hao et al., 2018).

Whole-rock major and trace elements

Major and trace element data are listed in Supplementary Table S2. The Sailipu high-K calc-alkaline lavas have relatively homogenous SiO_2 contents (56.9–59.6 wt.%) and total alkali (K_2O+Na_2O) contents (6.6–7.0 wt.%), plotting within the trachyandesite field (Figure 3A). The Sailipu trachyandesites show relatively low MgO (2.3–4.2 wt.%) contents and K_2O/Na_2O ratios (0.8–1.1), which are clearly different from the ultrapotassic rocks in the Lhasa block (Figures 3A-C). However, they have high CaO, TiO_2, TFe_2O_3, P_2O_5, and Y contents similar to those of ultrapotassic rocks (Figures 3D,F,H,I, 4C). They also differ from the adakitic rocks in the eastern Lhasa block by having lower SiO_2 and higher Y concentrations (Figures 3, 4C). On Harker diagrams (Figures 3E,G), the Sailipu trachyandesites generally plot between the fields of ultrapotassic rocks and late Cretaceous adakitic rocks in the western Lhasa block (e.g., Azhang adakites) (Sun et al., 2015). The ~90 Ma Azhang adakitic rocks were considered to represent the products of partial melting of the juvenile crust beneath the western Lhasa block (Sun et al., 2015).

On chondrite-normalized REE diagrams, the Sailipu trachyandesites are enriched in LREEs and depleted in HREEs (Figure 4A, Yb = 1.08–1.48 ppm, Y = 14.0–26.8 ppm), with $(La/Yb)_N$ and $(Dy/Yb)_N$ ratios of 33–55 and 1.9–2.2, respectively. They show slightly negative Eu anomalies (Eu/Eu* = 0.8–0.9). Their primitive mantle–normalized trace element distribution patterns are characterized by enrichment in large ion lithophile elements (LILEs) and depletion in high-field-strength elements (HFSEs), with negative Nb, Ta, Ti concentration anomalies and slightly negative to positive Sr anomaly (Figure 4B). On REE and trace element spider diagrams, the Sailipu trachyandesites plot in between the ultrapotassic rocks and the late Cretaceous adakitic rocks (Figures 4A,B).

Collectively, the Sailipu trachyandesites display adakitic affinities as defined by Defant and Drummond (1990), such as high SiO_2 (56.9–59.6 wt.%), Al_2O_3 (15.4–16.2 wt.%), and Sr (>1080 ppm) and low Yb (<1.5 ppm) and Y (mostly ≤18 ppm) contents, high Sr/Y (46–95) and La/Yb (46–77) ratios, enrichment in LREEs, and depletion in HREEs (Figures 4C,D).

Sr–Nd–B isotopic geochemistry

The Sailipu adakitic trachyandesites exhibit slightly high initial $^{87}Sr/^{86}Sr$ ratios (0.7092–0.7095) and low εNd(t) values

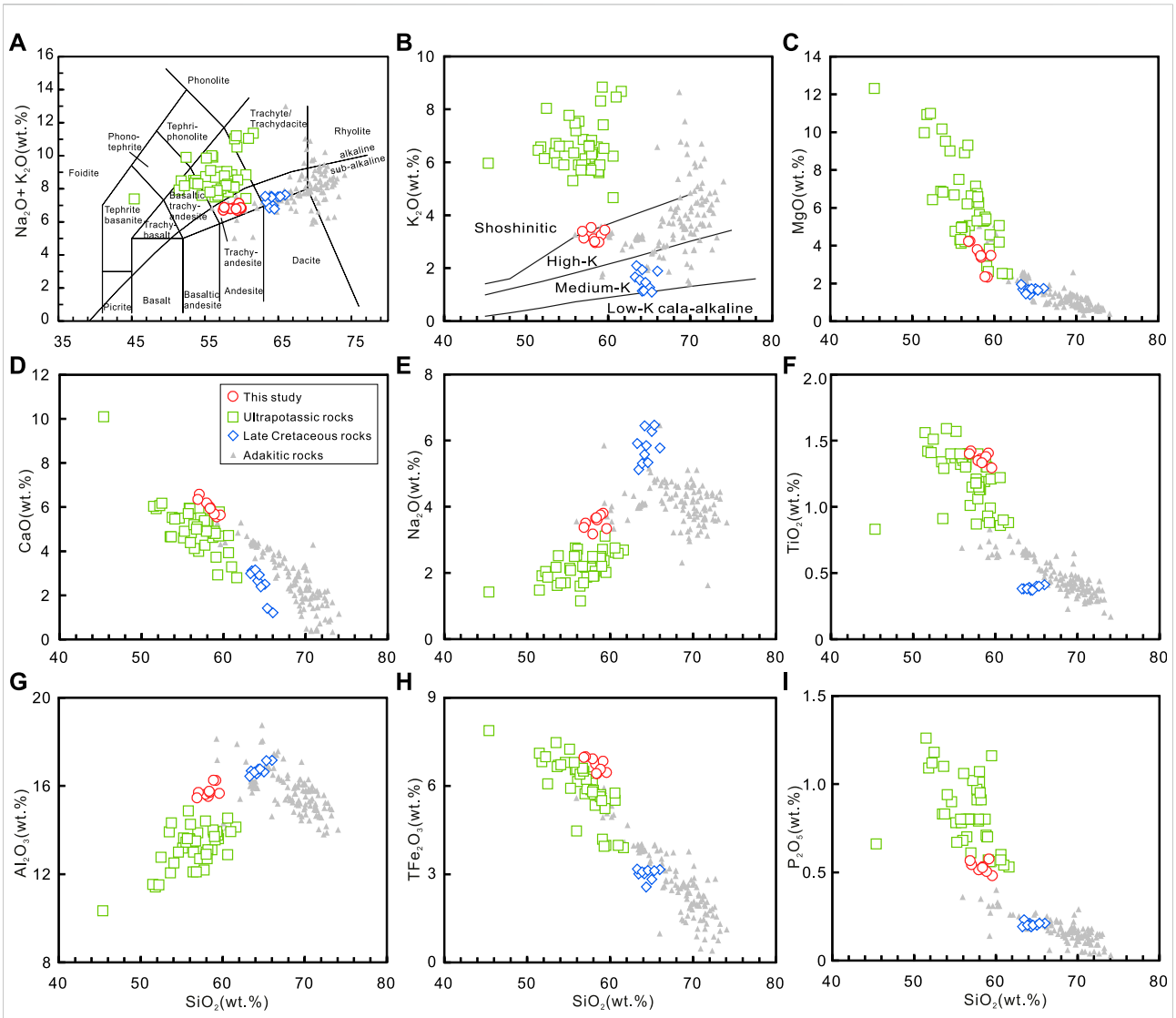

FIGURE 3
Major elemental compositions for Sailipu high-K calc-alkaline trachyandesites. **(A)** TAS diagram; **(B–I)** Harker diagrams. Data sources: adakitic rocks (Chung et al., 2003; Hou et al., 2004; Gao et al., 2007; Guo et al., 2007; Xu et al., 2010; Zheng et al., 2012; Ma et al., 2014; Yang et al., 2015; Liu et al., 2017); ultrapotassic rocks (Miller et al., 1999; Zhao et al., 2009; Liu et al., 2014); late Cretaceous magmatic rocks (Sun et al., 2015).

(−8.09 to −7.25) (Supplementary Table S2 and Figure 5). Their Sr–Nd isotopic compositions are more geochemically enriched than those of Cenozoic adakitic rocks in the eastern Lhasa block (e.g., Chung et al., 2003; Hou et al., 2004; Guo et al., 2007) and late Cretaceous juvenile crust–derived magmatic rocks in the western Lhasa block (Sun et al., 2015) (Figure 5). However, their Sr–Nd isotopic compositions are less geochemically enriched than those of ultrapotassic rocks in the Lhasa block (e.g., Guo et al., 2015; Liu et al., 2015; Tian et al., 2020).

Whole-rock B concentrations and isotopic compositions for the Sailipu adakitic trachyandesites are presented in Supplementary Table S2. They have low B concentrations (4.9–10.1 ppm) and show higher $\delta^{11}B$ values (−9.7 to −2.7‰) than MORBs ($\delta^{11}B = -7.1 \pm 0.9$‰, Marschall et al., 2017) and the average continental crust ($\delta^{11}B = -9.1 \pm 2.4$‰, Trumbull and Slack, 2017) (Figure 6A). Moreover, their $\delta^{11}B$ values are much higher than those of post-collisional ultrapotassic rocks in the Lhasa block (Hao et al., 2022). Instead, the B isotopic compositions of the Sailipu trachyandesites are similar to those of pre-collisional ultrapotassic rocks in the Rongniduo area of the Lhasa block ($\delta^{11}B = -9.0$‰ to −2.5‰, Hao et al., 2022) and modern arc magmas (De Hoog and Savov, 2017) (Figure 6A).

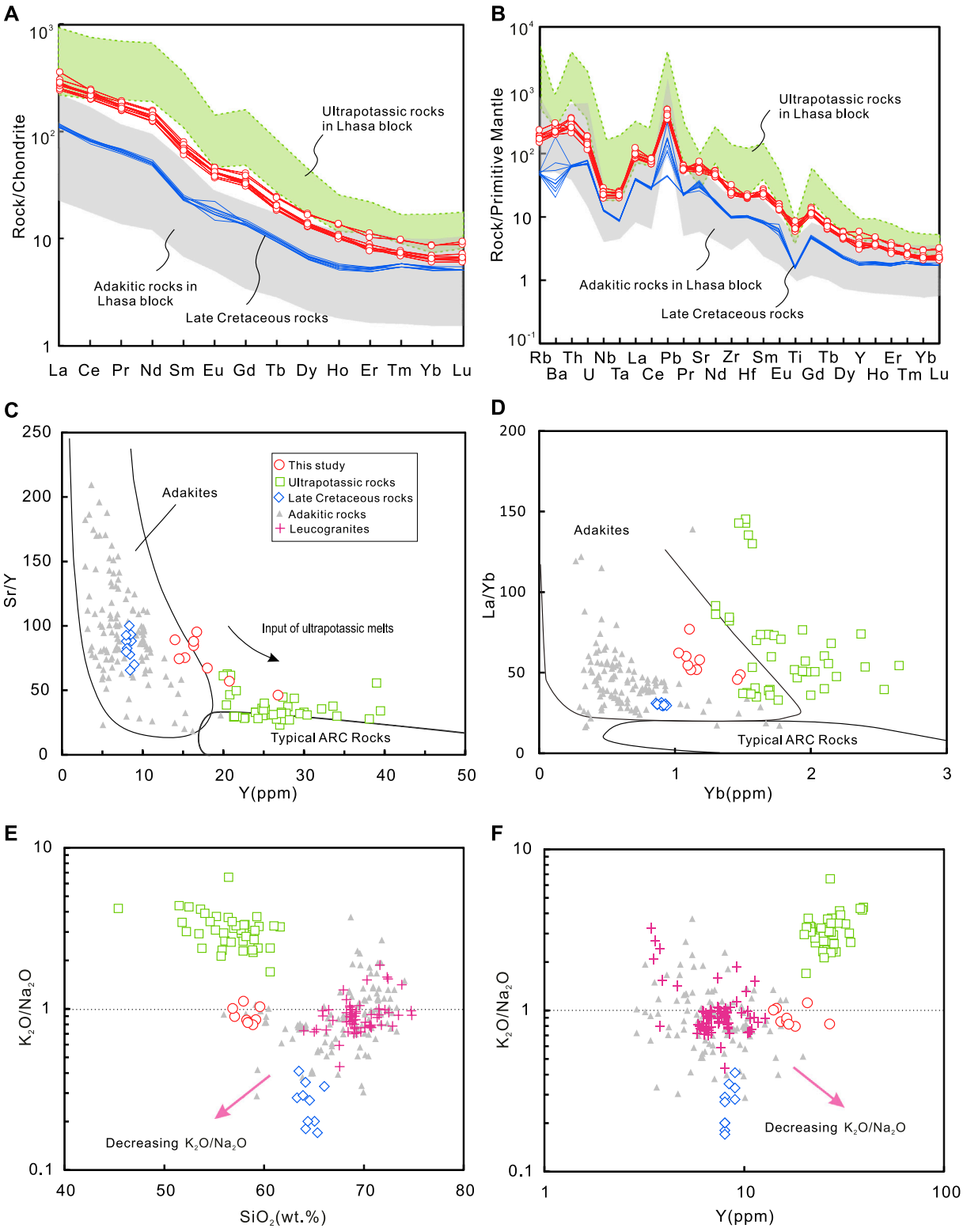

FIGURE 4
(A) Chondrite-normalized REE (rare earth element) and **(B)** primitive mantle–normalized trace element distribution patterns. **(C)** Sr/Y vs. Y. **(D)** La/Yb vs. Yb. **(E,F)** K_2O/Na_2O vs. SiO_2 and Y for Sailipu trachyandesites, respectively. The data sources of adakitic rocks, ultrapotassic rocks, and late Cretaceous magmatic rocks are the same as in Figure 3. The leucogranites are from Zeng et al. (2011), Hou et al. (2012), and Liu et al. (2014). Chondrite and primitive mantle values are from Sun and McDonough (1989).

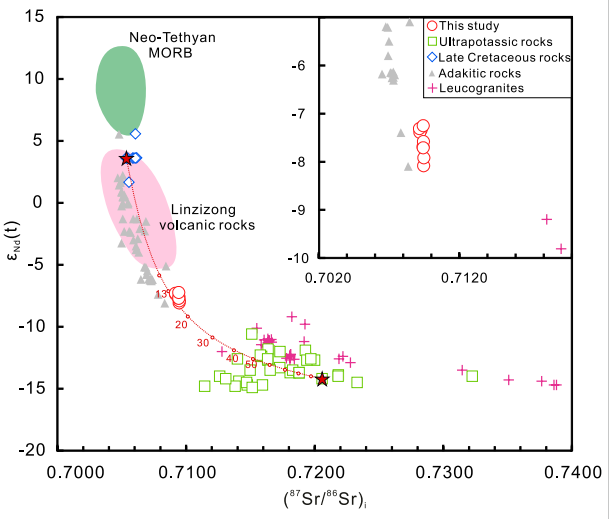

FIGURE 5
Initial Sr–Nd isotopic compositions for Sailipu trachyandesites. Data sources are the same as in Figure 4, Neo-Tethys MORBs (Xu and Castillo, 2004), and Linzizong volcanic rocks (Mo et al., 2007). The mixing endmembers are ultrapotassic rocks and late Cretaceous magmatic rocks representing the juvenile crust. The numbers (%) on the mixing curve represent the proportions of ultrapotassic magmas.

Discussions

A lower crust origin for adakitic trachyandesites

As noted above, the Sailipu trachyandesites show adakitic affinities. Previous studies (e.g., Castillo et al., 1999; Macpherson et al., 2006) have proposed that high-pressure fractional crystallization (±crustal contamination) of mafic magmas can produce adakitic rocks. Post-collisional mantle-derived ultrapotassic rocks are widely distributed in the western Lhasa block, yet significant geochemical differences occurred between the Sailipu trachyandesites and the ultrapotassic rocks: *1*) The Sailipu trachyandesites have low total alkali (K_2O+Na_2O) and K_2O contents and are sub-alkaline and high-K calc-alkaline, while the ultrapotassic rocks have much higher (K_2O+Na_2O) and K_2O contents (Figures 3A,B). *2*) The ultrapotassic rocks show higher Yb and Y contents and more geochemically enriched Sr–Nd isotopic compositions than the Sailipu trachyandesites (Figures 4C,D, 5). If a magma experienced the high-pressure fractional crystallization, a positive correlation between SiO_2 contents and Sr/Y and Dy/Yb ratios should be observed (Macpherson et al., 2006), yet the Sailipu trachyandesites do not show such correlations (Supplementary Figure S2). Therefore, the Sailipu trachyandesites were unlikely generated by fractional crystallization from ultrapotassic magmas.

Instead, the Sailipu adakitic trachyandesites have relatively high SiO_2 and low MgO contents, suggesting that they were likely produced by partial melting of thickened lower crust, similar to the origin of Cenozoic adakitic rocks in the eastern Lhasa block (e.g., Chung et al., 2003; Hou et al., 2004; Liu et al., 2017). However, the nature of their lower crust source remains unclear. Variable crustal components were suggested to contribute to their generation, including ancient lower crust (Liu et al., 2014; Hao et al., 2019a), subducted Indian continental crust (Xu et al., 2010; Liu et al., 2017), and juvenile lower crust (e.g., Hou et al., 2004; Yang et al., 2015).

Heavy B isotopic compositions indicate contributions of juvenile crust

Their petrographic features indicate that Sailipu adakitic trachyandesites are fresh (Supplementary Figure S1), consistent with their low loss on ignition values (LOI, < 0.9 wt.%). Thus, their B isotopic compositions most likely have not been affected by post-eruption alteration. Previous studies have shown that B isotopic ratios are insensitive to partial melting and fractional crystallization (Kasemann et al., 2000; Jones et al., 2014) because of the high incompatibility of B. Therefore, the B isotopic compositions of the Sailipu trachyandesites were inherited from their crustal origin.

The Sailipu adakitic trachyandesites have heavier B isotopic compositions than MORBs. Here, we suggest that these high $\delta^{11}B$ values could have not been sourced from the subducted Indian continental crust, ancient lower crust beneath the Lhasa block, or post-collisional ultrapotassic magmas. *1*) The two-mica schist and gneiss in the Tethyan Himalaya, which may represent the Indian continental crust, have extremely low $\delta^{11}B$ values of −19.5‰ and −22.1‰, respectively (Figure 6B) (Fan et al., 2021). Hu et al. (2018) also reported the light B isotopic compositions ($\delta^{11}B$ = −18.9 to −8.0‰) of tourmalines from metamorphic rocks and leucogranites in the Himalaya block. *2*) The $\delta^{11}B$ values of average continental crust are predicted to be −9.1 ± 2.4‰ (Trumbull and Slack, 2017). *3*) The post-collisional ultrapotassic rocks in the Lhasa block, considered to be derived from the low degree melting of the enriched lithospheric mantle, show very light B isotopic compositions ($\delta^{11}B$ = −20.5 to −10.3‰) (Hao et al., 2022).

Oceanic slab components, such as subducted sediments, altered oceanic crust, and serpentinited mantle, have heavy B isotopic compositions (De Hoog and Savov, 2017). Oceanic slab subduction triggers the generation of arc lavas and juvenile crust, which generally have heavy B isotopic compositions. This is because B-rich fluids with heavy B isotopic compositions are released from the subducted slab and then transferred into the sub-arc mantle wedge source of arc lavas. Modern arc lavas (continental arcs and island arcs, De Hoog and Savov, 2017 and intraplate basalts (Tonarini et al., 2004; Tonarini et al., 2005; Li et al., 2016; Zhang et al., 2019) generally have heavy B isotopic compositions (Figures 6A,B). Importantly, pre-collisional Rongniduo ultrapotassic rocks in the Lhasa block derived

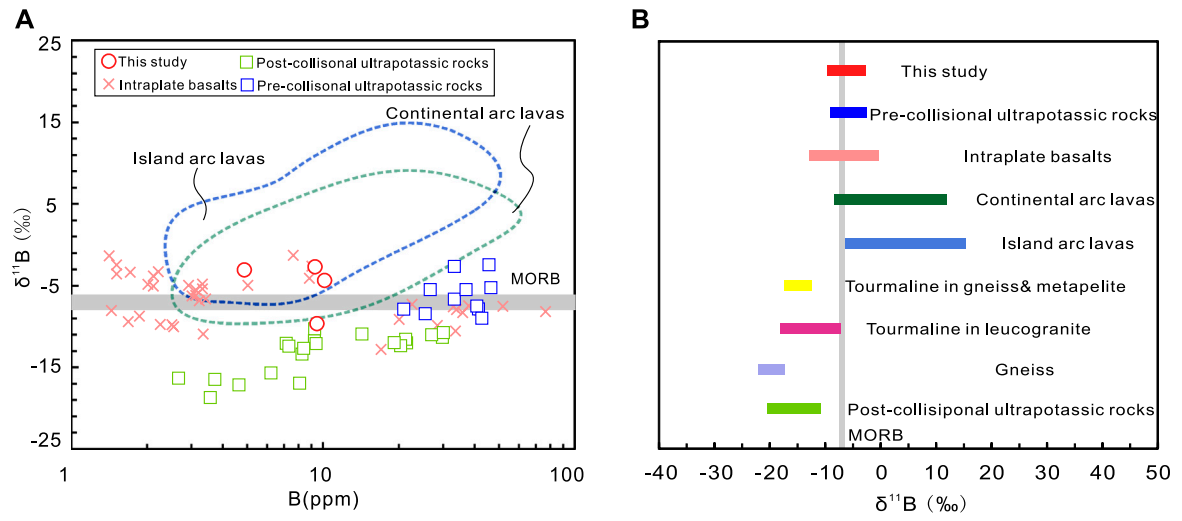

FIGURE 6
(A) Whole-rock $\delta^{11}B$ vs. B concentrations for Sailipu trachyandesites. **(B)** B isotopes for Sailipu trachyandesites and major reservoirs. Data source: intraplate basalts (Tonarini et al., 2004; Tonarini et al., 2005; Li et al., 2016; Zhang et al., 2019); arc lavas (island and continental arc lavas; De Hoog and Savov, 2017); tourmaline in gneiss and metapelite, leucogranites (Hu et al., 2018); schist and gneiss (Fan et al., 2021); pre-collisional and post-collisional ultrapotassic rocks in the Lhasa block (Hao et al., 2022). The gray fields for $\delta^{11}B$ of the MORBs are from Marschall et al. (2017).

from the metasomatized lithospheric mantle by Neo-Tethys oceanic subduction have arc-like heavy B isotopic compositions ($\delta^{11}B$ = −9.0 to −2.5‰) (Hao et al., 2022). The $\delta^{11}B$ values (−9.7 to −2.7‰) of the Sailipu trachyandesites are similar to those of the arc lavas and pre-collisional ultrapotassic rocks, suggesting significant contributions of juvenile crust to their generation.

Geochemically enriched Sr–Nd isotopes sourced from ultrapotassic magmas

The late Cretaceous adakitic magmatism in the western Lhasa block (e.g., Azhang adakites) was considered to be produced by partial melting of the juvenile lower crust (Sun et al., 2015; Lei et al., 2019). However, compared to these late Cretaceous magmatic rocks, the Sailipu adakitic trachyandesites have lower SiO_2 contents, higher Sr, Ba concentrations, and more geochemically enriched Sr–Nd isotopes (Figure 5). These signatures cannot be explained by a sole juvenile lower crustal origin. We favor a magma mixing model between the juvenile lower crust (isotopically depleted) and an isotope-enriched endmember to account for the formation of Sailipu adakitic trachyandesites.

In the broad context of Indian continental subduction beneath the Lhasa block, Indian continental crust, ancient lower crust, and post-collisional ultrapotassic magmas can be the potential geochemically enriched endmembers (e.g., Guo et al., 2007; Xu et al., 2010; Liu et al., 2014; Liu et al., 2017; Hao et al., 2019a). However, the subducted Indian continental crust should contribute insignificantly to the Sailipu trachyandesites. The Tethyan Himalayan leucogranites [$(^{87}Sr/^{86}Sr)_i$ = 0.7155–0.7193, $\varepsilon_{Nd}(t)$ = −9.2 to −13.3] were generally interpreted to be derived from anatexis of Indian continental crust (Zeng et al., 2011; Hou et al., 2012). For these leucogranites, the decreasing K_2O/Na_2O is coupled with reduced SiO_2 and increased Y concentrations (Figures 4E,F). The involvement of Indian crust with the juvenile lower crust fails to produce the Sailipu trachyandesites. Similarly, the involvement of thickened ancient lower crust is also unlikely to explain the higher Y contents of the Sailipu trachyandesites than Azhang adakites.

Another possible mechanism responsible for evolved Sr–Nd isotopes and high Y concentrations would be coeval ultrapotassic magmas. The relatively high MgO (2.3–4.2 wt.%), Cr (90–118 ppm), and Ni (52–101 ppm) contents of the Sailipu trachyandesites require a mafic component in the source, which is consistent with the input of ultrapotassic melts (e.g., Liu et al., 2014; Guo et al., 2015). Miocene coeval ultrapotassic lavas are exposed in the western Lhasa block (e.g., ~24 Ma in the Xungba basin, Miller et al., 1999; Liu et al., 2011) (Figure 1) and have high MgO, K_2O, and TiO_2 contents (Figure 3) and extremely enriched Sr–Nd isotopic compositions [$(^{87}Sr/^{86}Sr)_i$ = 0.7115–0.7323, $\varepsilon_{Nd}(t)$ = −14.9 to −10.6] (Figure 5). The Sailipu trachyandesites have CaO and TiO_2 contents similar to those of the ultrapotassic rocks (Figures 3D,H). In the plots of MgO and K_2O/Na_2O versus SiO_2 and K_2O/Na_2O versus Y, the Sailipu trachyandesites are intermediate between the late Cretaceous Azhang adakites and the ultrapotassic rocks (Figures 3C, 4E,F).

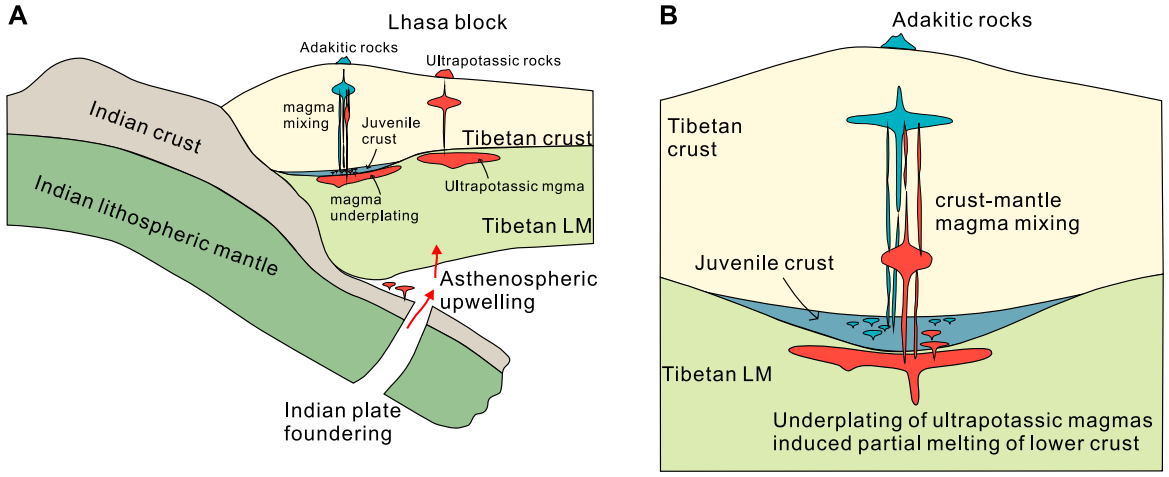

FIGURE 7
(A) Schematic illustration for the formation of adakitic trachyandesites. **(B)** Schematic model for the interaction of ultrapotassic magmas with lower crust. LM, lithospheric mantle. The subducted Indian continental plate experienced foundering, which triggered the asthenosphere upwelling and partial melting of metasomatized lithospheric mantle to generate ultrapotassic magmas. The underplating of ultrapotassic magmas beneath the lower crust of the Lhasa block induced partial melting of the juvenile lower crust. Mixing between the juvenile lower crust–derived melts and the ultrapotassic magmas formed the Sailipu high-K calc-alkaline and adakitic trachyandesites.

The same scenarios are also observed on the REE and trace element distribution diagrams (Figures 4A,B). The input of high-Y ultrapotassic melts can well explain some samples outside of the adakite region in the plot of Sr/Y versus Y (Figure 4C). Furthermore, model mixing curves between the juvenile lower crust and 13–17% ultrapotassic melts can fully account for the Sr–Nd isotopic compositions of the Sailipu trachyandesites (Figure 5).

Overall, the geochemical, isotopic, and temporal–spatial evidence suggests that the Sailipu adakitic trachyandesites were produced by magma mixing between mantle-derived ultrapotassic magmas and juvenile lower crust–derived melts.

Implications for crustal reworking in southern Tibet during Indian continental subduction

Continental collisional zones are important locations for crustal reworking. The Himalayan–Tibetan orogen, built by India–Asia collision and Indian continental plate subduction, is underlain by the thickest continental crust on Earth and is one of the best places to study the mechanism of crustal reworking. Numerous studies on the adakitic rocks in the eastern Lhasa block have suggested that these rocks were derived from magma mixing between juvenile crust–derived melts and post-collisional mantle-derived ultrapotassic magmas (e.g., Yang et al., 2015; Wang et al., 2018; Hao et al., 2021). This indicates that underplating of ultrapotassic magmas induced the reworking of juvenile crust in the eastern Lhasa block. A similar scenario was studied by Hao et al. (2019a), who suggested that the Miocene Konglong potassic trachytes in the central Lhasa block were generated by mantle–crust mixing. This means that magma underplating and subsequent crust–mantle mixing played an important role in crustal reworking. However, the adakitic rocks in the western Lhasa block draw much less attention, and their genesis remains unclear, hindering our understanding of the mechanism of crustal reworking in southern Tibet.

In this study, B–Sr–Nd isotopes reveal that the adakitic trachyandesites from the Sailipu basin in the western Lhasa block were derived from partial melting of a juvenile crust with contributions from post-collisional mantle-derived ultrapotassic magmas. Previous studies have suggested that following the initial Lhasa–Himalaya collision in the early Cenozoic (Hu et al., 2015) and the break-off of Neo-Tethyan oceanic slab at ~50–45 Ma, the Indian continental plate began to northwardly subduct beneath the Lhasa block. The subducted Indian continental plate then experienced slab foundering and tearing since ~25 Ma (Hao et al., 2019b), which triggered the asthenosphere upwelling and partial melting of lithospheric mantle. The mantle-derived ultrapotassic magmas could have underplated beneath the lower crust of the Lhasa block, resulting in partial melting of the lower crust. Mixing between the juvenile lower crust–derived melts and the ultrapotassic magmas formed the Sailipu high-K calc-alkaline and adakitic trachyandesites (Figure 7).

Collectively, the Sailipu trachyandesites in the western Lhasa block, combined with post-collisional adakitic magmatism in the eastern Lhasa block and Konglong potassic trachytes in the central Lhasa block, suggest that underplating of mantle-derived ultrapotassic magma and subsequent crust–mantle magma mixing were a common and important process that induced crustal reworking in southern Tibet during Indian continental

subduction. The ultrapotassic magmas significantly contributed to this crustal reworking through energy and mass transfer.

Conclusion

1) The Miocene high-K calc-alkaline trachyandesites from the Sailipu basin in the western Lhasa block show adakitic affinities and geochemically enriched Sr–Nd and heavy B isotopic compositions.
2) Their arc-like heavy B isotopic compositions indicate contributions of juvenile crust. Their geochemically enriched Sr–Nd isotopes, combined with high TiO_2 and Y contents, likely suggest input from ultrapotassic magmas.
3) Underplating of ultrapotassic magmas and subsequent mantle–crust interaction could be a common process leading to crustal reworking in southern Tibet.

Data availability statement

The original contributions presented in the study are included in the article/Supplementary Material, and further inquiries can be directed to the corresponding authors.

Author contributions

L-LH and YQ jointly proposed the research plan. L-LH, QW, and LM collected the rock samples. M-YZ conducted the analyses. M-YZ, L-LH, QW, YQ, and LM comprehensively interpreted the geochemical data. M-YZ, L-LH, and YQ drafted the primary paper. QW and LM contributed to improving the writing of this paper.

Funding

This study was financially supported by the National Natural Science Foundation of China (NSFC) (91855215, 42021002, and 42073025), Youth Innovation Promotion Association, CAS (2022357), and Guangzhou Science and Technology Program: Basic and Applied Basic Research Project (202102020925). This is contribution No.IS-3220 from GIGCAS.

Acknowledgments

We are very grateful to the editor Hossein Azizi and two reviewers for their detailed and constructive comments which greatly improved the manuscript. We appreciate the assistance of Ya-Nan Yang, Miao-Hong He, Xin-Yu Wang, Xiang-Lin Tu, and Sheng-Ling Sun for zircon age and whole-rock major and trace element analyses. Wen Zeng, Jin-Long Ma, and Le Zhang are thanked for their help with Sr–Nd–B isotope analyses.

Conflict of interest

The authors declare that the research was conducted in the absence of any commercial or financial relationships that could be construed as a potential conflict of interest.

Publisher's note

All claims expressed in this article are solely those of the authors and do not necessarily represent those of their affiliated organizations, or those of the publisher, the editors, and the reviewers. Any product that may be evaluated in this article, or claim that may be made by its manufacturer, is not guaranteed or endorsed by the publisher.

Supplementary material

The Supplementary Material for this article can be found online at: https://www.frontiersin.org/articles/10.3389/feart.2022.953364/full#supplementary-material

References

Castillo, P. R. (2012). Adakite petrogenesis. *Lithos* 134–135, 304–316. doi:10.1016/j.lithos.2011.09.013

Castillo, P. R., Janney, P. E., and Solidum, R. U. (1999). Petrology and geochemistry of Camiguin island, southern Philippines: insights to the source of adakites and other lavas in a complex arc setting. *Contrib. Mineral. Petrol.* 134, 33–51. doi:10.1007/s004100050467

Chen, J., Xu, J., Wang, B., and Kang, Z. (2012). Cenozoic Mg-rich potassic rocks in the Tibetan plateau: geochemical variations, heterogeneity of subcontinental lithospheric mantle and tectonic implications. *J. Asian Earth Sci.* 53, 115–130. doi:10.1016/j.jseaes.2012.03.003

Cheng, Z., and Guo, Z. (2017). Post-collisional ultrapotassic rocks and mantle xenoliths in the Sailipu volcanic field of Lhasa terrane, south Tibet: petrological and geochemical constraints on mantle source and geodynamic setting. *Gondwana Res.* 46, 17–42. doi:10.1016/j.gr.2017.02.008

Chung, S. L., Chu, M. F., Ji, J., O'Reilly, S. Y., Pearson, N., Liu, D., et al. (2009). The nature and timing of crustal thickening in southern Tibet: geochemical and zircon Hf isotopic constraints from postcollisional adakites. *Tectonophysics* 477, 36–48. doi:10.1016/j.tecto.2009.08.008

Chung, S. L., Chu, M. F., Zhang, Y., Xie, Y., Lo, C. H., Lee, T. Y., et al. (2005). Tibetan tectonic evolution inferred from spatial and temporal variations in post-collisional magmatism. *Earth-Sci. Rev.* 68, 173–196. doi:10.1016/j.earscirev.2004.05.001

Chung, S. L., Liu, D., Ji, J., Chu, M. F., Lee, H. Y., Wen, D. J., et al. (2003). Adakites from continental collision zones: melting of thickened lower crust beneath southern Tibet. *Geology* 31, 1021. doi:10.1130/g19796.1

De Hoog, J., and Savov, I. P. (2017). "Boron isotopes as a tracer of subduction zone processes," in *Boron isotopes: the fifth element*. Editors H. Marschall and G. Foster (Cham, Switzerland: Springer Nature), 217–247.

Defant, M. J., and Drummond, M. S. (1990). Derivation of some modern arc magmas by melting of young subducted lithosphere. *Nature* 347, 662–665. doi:10.1038/347662a0

Fan, J. J., Wang, Q., Li, J., Wei, G. J., Ma, J. L., Ma, L., et al. (2021). Boron and molybdenum isotopic fractionation during crustal anatexis: Constraints from the Conadong leucogranites in the Himalayan block, South Tibet. *Geochim. Cosmochim. Acta* 297, 120–142. doi:10.1016/j.gca.2021.01.005

Gao, Y., Hou, Z., Kamber, B. S., Wei, R., Meng, X., Zhao, R., et al. (2007). Adakite-like porphyries from the southern Tibetan continental collision zones: evidence for slab melt metasomatism. *Contrib. Mineral. Pet.* 153, 105–120. doi:10.1007/s00410-006-0137-9

Guo, Z., Wilson, M., and Liu, J. (2007). Post-collisional adakites in south Tibet: products of partial melting of subduction-modified lower crust. *Lithos* 96, 205–224. doi:10.1016/j.lithos.2006.09.011

Guo, Z., Wilson, M., Zhang, M., Cheng, Z., and Zhang, L. (2015). Post-collisional ultrapotassic mafic magmatism in south Tibet: products of partial melting of pyroxenite in the mantle wedge induced by roll-back and delamination of the subducted Indian continental lithosphere slab. *J. Pet.* 56, 1365–1406. doi:10.1093/petrology/egv040

Guo, Z., Wilson, M., Zhang, M., Cheng, Z., and Zhang, L. (2013). Post-collisional, K-rich mafic magmatism in south Tibet: constraints on Indian slab-to-wedge transport processes and plateau uplift. *Contrib. Mineral. Pet.* 165 (6), 1311–1340. doi:10.1007/s00410-013-0860-y

Hao, L. L., Wang, Q., Kerr, A. C., Wei, G. J., Huang, F., Zhang, M. Y., et al. (2022). Contribution of continental subduction to very light B isotope signatures in post-collisional magmas: evidence from southern Tibetan ultrapotassic rocks. *Earth Planet. Sci. Lett.* 584, 117508. doi:10.1016/j.epsl.2022.117508

Hao, L. L., Wang, Q., Kerr, A. C., Yang, J. H., Ma, L., Qi, Y., et al. (2021). Post-collisional crustal thickening and plateau uplift of southern Tibet: insights from cenozoic magmatism in the wuyu area of the eastern Lhasa block. *Geol. Soc. Am. Bull.* 133 (7-8), 1634–1648. doi:10.1130/B35659.1

Hao, L. L., Wang, Q., Wyman, D. A., Ma, L., Wang, J., Xia, X. P., et al. (2019b). First identification of postcollisional A-type magmatism in the Himalayan-Tibetan orogen. *Geology* 47 (2), 187–190. doi:10.1130/g45526.1

Hao, L. L., Wang, Q., Wyman, D. A., Qi, Y., Ma, L., Huang, F., et al. (2018). First identification of mafic igneous enclaves in Miocene lavas of southern Tibet with implications for Indian continental subduction. *Geophys. Res. Lett.* 45 (16), 8205–8213. doi:10.1029/2018gl079061

Hao, L. L., Wang, Q., Wyman, D. A., Yang, J. H., Huang, F., Ma, L., et al. (2019a). Crust-mantle mixing and crustal reworking of southern Tibet during Indian continental subduction: evidence from Miocene high-silica potassic rocks in central Lhasa block. *Lithos* 342-343, 407–419. doi:10.1016/j.lithos.2019.05.035

Hou, Z. Q., Gao, Y. F., Qu, X. M., Rui, Z. Y., and Mo, X. X. (2004). Origin of adakitic intrusives generated during mid-Miocene east–west extension in southern Tibet. *Earth Planet. Sci. Lett.* 220, 139–155. doi:10.1016/s0012-821x(04)00007-x

Hou, Z. Q., Zheng, Y. C., Zeng, L. S., Gao, L. E., Huang, K. X., Li, W., et al. (2012). Eocene–oligocene granitoids in southern Tibet: constraints on crustal anatexis and tectonic evolution of the himalayan orogen. *Earth Planet. Sci. Lett.* 349, 38–52. doi:10.1016/j.epsl.2012.06.030

Hu, G., Zeng, L., Gao, L., Liu, Q., Chen, H., Guo, Y., et al. (2018). Diverse magma sources for the himalayan leucogranites: evidence from B-Sr-Nd isotopes. *Lithos* 314–315, 88–99. doi:10.1016/j.lithos.2018.05.022

Hu, X., Garzanti, E., Moore, T., and Raffi, I. (2015). Direct stratigraphic dating of India-Asia collision onset at the Selandian (middle Paleocene, 59 ± 1 Ma). *Geology* 43 (10), 859–862. doi:10.1130/g36872.1

Jones, R. E., De Hoog, J. C. M., Kirstein, L. A., Kasemann, S., Hinton, R., Elliot, T., et al. (2014). Temporal variations in the influence of the subducting slab on central Andean arc magmas: Evidence from boron isotope systematics. *Earth Planet. Sci. Lett.* 408, 390–401. doi:10.1016/j.epsl.2014.10.004

Kasemann, S., Erzinger, J., and Franz, G. (2000). Boron recycling in the continental crust of the central Andes from the Palaeozoic to Mesozoic, NW Argentina. *Contrib. Mineral. Pet.* 140 (3), 328–343. doi:10.1007/s004100000189

Lei, M., Chen, J. L., Xu, J. F., Zeng, Y. C., and Xiong, Q. W. (2019). Late Cretaceous magmatism in the NW Lhasa Terrane, southern Tibet: Implications for crustal thickening and initial surface uplift. *GSA Bull.* 132, 334–352. doi:10.1130/b31915.1

Li, H. Y., Zhou, Z., Ryan, J. G., Wei, G. J., and Xu, Y. G. (2016). Boron isotopes reveal multiple metasomatic events in the mantle beneath the eastern North China Craton. *Geochim. Cosmochim. Acta* 194, 77–90. doi:10.1016/j.gca.2016.08.027

Li, X. H., Liu, Y., Li, Q. L., Guo, C. H., and Chamberlain, K. R. (2009). Precise determination of Phanerozoic zircon Pb/Pb age by multicollector SIMS without external standardization. *Geochem. Geophys. Geosyst.* 10, Q04010. doi:10.1029/2009gc002400

Li, X., Li, Z., Wingate, M. T. D., Chung, S., Liu, Y., Lin, G., et al. (2006). Geochemistry of the 755 Ma mundine well dyke swarm, northwestern Australia: Part of a neoproterozoic mantle superplume beneath rodinia? *Precambrian Res.* 146 (1-2), 1–15. doi:10.1016/j.precamres.2005.12.007

Li, X., Liu, D., Sun, M., Li, W., Liang, X., Liu, Y., et al. (2004). Precise Sm-Nd and U-Pb isotopic dating of the supergiant shizhuyuan polymetallic deposit and its host granite, SE China. *Geol. Mag.* 141 (2), 225–231. doi:10.1017/s0016756803008823

Li, X., Qi, C., Liu, Y., Liang, X., Tu, X., Xie, L., et al. (2005). Petrogenesis of the neoproterozoic bimodal volcanic rocks along the Western margin of the yangtze block: new constraints from Hf isotopes and Fe/Mn ratios. *Chin. Sci. Bull.* 50, 2481. doi:10.1360/982005-287

Li, X., Tang, G., Gong, B., Yang, Y., Hou, K., Hu, Z., et al. (2013). Qinghu zircon: a working reference for microbeam analysis of U-Pb age and Hf and O isotopes. *Chin. Sci. Bull.* 58, 4647–4654. doi:10.1007/s11434-013-5932-x

Liu, D., Zhao, Z., Depaolo, D. J., Zhu, D., Meng, F., Shi, Q., et al. (2017). Potassic volcanic rocks and adakitic intrusions in southern Tibet: insights into mantle-crust interaction and mass transfer from Indian plate. *Lithos* 268–271, 48–64. doi:10.1016/j.lithos.2016.10.034

Liu, D., Zhao, Z. D., Zhu, D. C., Wang, Q., Sui, Q. L., Liu, Y. S., et al. (2011). The petrogenesis of post-collisional potassic–ultrapotassic rocks in Xungba basin, Western Lhasa terrane: constraints from zircon U–Pb geochronology and geochemistry. *Acta Petrol. Sin.* 27, 2045–2059. (in Chinese with English abstract). doi:10.1016/S1002-0160(11)60127-6

Liu, D., Zhao, Z., Zhu, D. C., Niu, Y., Depaolo, D. J., Harrison, T. M., et al. (2014). Postcollisional potassic and ultrapotassic rocks in southern Tibet: mantle and crustal origins in response to India-asia collision and convergence. *Geochim. Cosmochim. Acta* 143 (27), 207–231. doi:10.1016/j.gca.2014.03.031

Liu, D., Zhao, Z., Zhu, D. C., Niu, Y., Widom, E., Teng, F., et al. (2015). Identifying mantle carbonatite metasomatism through Os-Sr-Mg isotopes in Tibetan ultrapotassic rocks. *Earth Planet. Sci. Lett.* 430, 458–469. doi:10.1016/j.epsl.2015.09.005

Ma, L., Wang, B. D., Jiang, Z. Q., Wang, Q., Li, Z. X., Wyman, D. A., et al. (2014). Petrogenesis of the early Eocene adakitic rocks in the Napuri area, southern Lhasa: Partial melting of thickened lower crust during slab break-off and implications for crustal thickening in southern Tibet. *Lithos* 196–197, 321–338. doi:10.1016/j.lithos.2014.02.011

Macpherson, C. G., Dreher, S. T., and Thirlwall, M. F. (2006). Adakites without slab melting: high pressure differentiation of island arc magma, mindanao, the Philippines. *Earth Planet. Sci. Lett.* 243, 581–593. doi:10.1016/j.epsl.2005.12.034

Marschall, H. R. (2017). "Boron isotopes in the ocean floor realm and the mantle," in *Boron isotopes: the fifth element*. Editors H. R. Marschall and G. L. Foster (Cham, Switzerland: Springer Nature), 189–215.

Marschall, H. R., Wanless, V. D., Shimizu, N., Pogge von Strandmann, P. A. E., Elliott, T., Monteleone, B. D., et al. (2017). The boron and lithium isotopic composition of mid-ocean ridge basalts and the mantle. *Geochim. Cosmochim. Acta* 207, 102–138. doi:10.1016/j.gca.2017.03.028

Miller, C., Schuster, R., Klötzli, U., Frank, W., and Purtscheller, F. (1999). Post-collisional potassic and ultrapotassic magmatism in SW Tibet: geochemical and Sr-Nd-Pb-O isotopic constraints for mantle source characteristics and petrogenesis. *J. Petrol.* 40, 1399–1424. doi:10.1093/petroj/40.9.1399

Mo, X., Hou, Z., Niu, Y., Dong, G., Qu, X., Zhao, Z., et al. (2007). Mantle contributions to crustal thickening during continental collision: evidence from cenozoic igneous rocks in southern Tibet. *Lithos* 96 (1), 225–242. doi:10.1016/j.lithos.2006.10.005

Palmer, M. R., Ersoy, E. Y., Akal, C., Uysal, i., Genç, Ş. C., Banks, L. A., et al. (2019). A short, sharp pulse of potassium-rich volcanism during continental collision and subduction. *Geology* 47 (11), 1079–1082. doi:10.1130/g45836.1

Sun, S., and McDonough, W. F. (1989). "Chemical and isotopic systematics of oceanic basalts: implications for mantle composition and processes," in *Magmatismin the ocean basins. Geological society*. Editors A. D. Saunders and M. J. Norry (London: Special Publications), 42, 313–345.

Sláma, J., Košler, J., Condon, D. J., Crowley, J. L., Gerdes, A., Hanchar, J. M., et al. (2008). Plešovice zircon—a new natural reference material for U–Pb and Hf isotopic microanalysis. *Chem. Geol.* 249, 1–35. doi:10.1016/j.chemgeo.2007.11.005

Sun, G. Y., Hu, X. M., Zhu, D. C., Hong, W. T., Wang, J. G., Wang, Q., et al. (2015). Thickened juvenile lower crust-derived ~90Ma adakitic rocks in the central Lhasa terrane, Tibet. *Lithos* 224-225, 225–239. doi:10.1016/j.lithos.2015.03.010

Tian, S., Hou, A., Mo, X., Tian, Y., Zhao, Y., Hou, K., et al. (2020). Lithium isotopic evidence for subduction of the Indian lower crust beneath southern Tibet. *Gondwana Res.* 77, 168–183. doi:10.1016/j.gr.2019.07.016

Tonarini, S., Agostini, S., Innocenti, F., and Manetti, P. (2005). delta11B as tracer of slab dehydration and mantle evolution in Western Anatolia Cenozoic Magmatism. *Terra Nova* 17 (3), 259–264. doi:10.1111/j.1365-3121.2005.00610.x

Tonarini, S., Leeman, W. P., Civetta, L., D'Antonio, M., Ferrara, G., Necco, A., et al. (2004). B/Nb and ^{11}B systematics in the phlegrean volcanic district, Italy. *J. Volcanol. Geotherm. Res.* 133 (1/4), 123–139. doi:10.1016/s0377-0273(03)00394-9

Trumbull, R. B., and Slack, J. F. (2017). "Boron isotopes in the continental crust: Granites, pegmatites, felsic volcanic rocks, and related ore deposits," in *Boron isotopes: the fifth element. Advances in isotope Geochemistry*. Editors H. R. Marschall and G. L. Foster (Cham: Springer), 249–272.

Wang, B., Chen, J., Xu, J., and Wang, L. (2014). Geochemical and Sr-Nd-Pb-Os isotopic compositions of Miocene ultrapotassic rocks in southern Tibet: Petrogenesis and implications for the regional tectonic history. *Lithos* 208-209, 237–250. doi:10.1016/j.lithos.2014.09.008

Wang, B., Xu, J., Zhang, X., Chen, J., Kang, Z., and Dong, Y. (2008). Petrogenesis of miocenevolcanic rocks in the Sailipu area, Western Tibetan plateau: geochemical and Sr–Nd isotopic constrains. *Acta Petrol. Sin.* 24, 265–278. (in Chinese with English abstract). doi:10.1016/j.sedgeo.2007.12.008

Wang, Q., McDermott, F., Xu, J. F., Bellon, H., and Zhu, Y. T. (2005). Cenozoic K-rich adakitic volcanic rocks in the hohxil area, northern Tibet: lower crustal melting in an intracontinental setting. *Geology* 33, 465. doi:10.1130/g21522.1

Wang, R., Weinberg, R. F., Collins, W. J., Richards, J. P., and Zhu, D. (2018). Origin of postcollisional magmas and formation of porphyry Cu deposits in southern Tibet. *Earth-Sci. Rev.* 181, 122–143. doi:10.1016/j.earscirev.2018.02.019

Wei, G., Wei, J., Liu, Y., Ke, T., Ren, Z., Ma, J., et al. (2013). Measurement on high precision boron isotope of silicate materials by a single column purification method and MC-ICP-MS. *J. Anal. At. Spectrom.* 28, 606. doi:10.1039/c3ja30333k

Weis, D., Kieffer, B., Maerschalk, C., Pretorius, W., and Barling, J. (2005). High-precision Pb-Sr-Nd-Hf isotopic characterization of USGS BHVO-1 and BHVO-2 reference materials. *Geochem. Geophys. Geosyst.* 6, Q02002. doi:10.1029/2004gc000852

Xu, J. F., and Castillo, P. R. (2004). Geochemical and Nd–Pb isotopic characteristics of the tethyan asthenosphere: implications for the origin of the Indian ocean mantle domain. *Tectonophysics* 393, 9–27. doi:10.1016/j.tecto.2004.07.028

Xu, W. C., Zhang, H. F., Guo, L., and Yuan, H. L. (2010). Miocene high Sr/Y magmatism, south Tibet: product of partial melting of subducted Indian continental crust and its tectonic implication. *Lithos* 114, 293–306. doi:10.1016/j.lithos.2009.09.005

Yang, Z. M., Lu, Y. J., Hou, Z. Q., and Chang, Z. S. (2015). High-Mg diorite from qulong in southern Tibet: implications for the Genesis of adakite-like intrusions and associated porphyry Cu deposits in collisional orogens. *J. Petrology* 56, 227–254. doi:10.1093/petrology/egu076

Yin, A., and Harrison, T. M. (2000). Geologic evolution of the Himalayan–Tibetan orogen. *Annu. Rev. Earth Planet. Sci.* 28, 211–280. doi:10.1146/annurev.earth.28.1.211

Zeng, L., Gao, L. E., Xie, K., and Jing, L. Z. (2011). Mid-eocene high Sr/Y granites in the northern himalayan gneiss domes: melting thickened lower continental crust. *Earth Planet. Sci. Lett.* 303, 251–266. doi:10.1016/j.epsl.2011.01.005

Zhang, Y., Yuan, C., Sun, M., Chen, M., Hong, L., Li, J., et al. (2019). Recycled oceanic crust in the form of pyroxenite contributing to the cenozoic continental basalts in central asia: new perspectives from olivine chemistry and whole-rock B-Mo isotopes. *Contrib. Mineral. Pet.* 178, 83. doi:10.1007/s00410-019-1620-4

Zhao, Z., Mo, X., Dilek, Y., Niu, Y., Depaolo, D. J., Robinson, P., et al. (2009). Geochemical and Sr-Nd-Pb-O isotopic compositions of the post-collisional ultrapotassic magmatism in SW Tibet: petrogenesis and implications for India intra-continental subduction beneath southern Tibet. *Lithos* 113 (1-2), 190–212. doi:10.1016/j.lithos.2009.02.004

Zheng, Y. C., Hou, Z.-Q., Li, Q. Y., Sun, Q. Z., Liang, W., Fu, Q., et al. (2012). Origin of late Oligocene adakitic intrusives in the southeastern Lhasa terrane: evidence from *in situ* zircon U–Pb dating, Hf–O isotopes, and whole-rock geochemistry. *Lithos* 148, 296–311. doi:10.1016/j.lithos.2012.05.026

Zhu, D., Zhao, Z., Niu, Y., Dilek, Y., Hou, Z., Mo, X., et al. (2013). The origin and pre-Cenozoic evolution of the Tibetan plateau. *Gondwana Res.* 23 (4), 1429–1454. doi:10.1016/j.gr.2012.02.002

Zhu, D., Zhao, Z., Niu, Y., Mo, X., Wu, F., Hou, Z. Q., et al. (2011). The Lhasa Terrane: Record of a microcontinent and its histories of drift and growth. *Earth Planet. Sci. Lett.* 301 (1), 241–255. doi:10.1016/j.epsl.2010.11.005